

Electronic Supplementary Information (ESI)

A self-healing Li-S redox flow battery with alternative reaction pathways

Qiliang Chen,^a Wei Guo,^a Donghai Wang^b and Yongzhu Fu^{*a}

^a *College of Chemistry, Zhengzhou University, Zhengzhou 450001, P. R. China*

^b *Department of Mechanical Engineering, The Pennsylvania State University, University Park, PA 16802, USA*

Experimental section

Chemicals. Dimethoxyethane (DME) and 1,3-dioxolane (DOL) (1:1 by volume) with 1.0 M lithium bis(trifluoromethanesulfonyl)imide (LiTFSI) and 0.3 M lithium nitrate (LiNO₃) as the supporting electrolyte, which was received from Canrd. Graphite felt with a thickness of about 3 mm was purchased from Dalian Longtian Tech Co., Ltd. Carbon paper was purchased from NanoTechLabs Composites, Inc. Lithium metal foil was purchased from China Energy Lithium Co., Ltd. 2,2'-dipyridyl disulfide (PySSPy, 98%) was purchased from TCI Chemicals. Diphenyl diselenide (PhSeSePh, 99%,) was purchased from Acros. The sulfur powder was purchased from Aladdin. For the other chemicals, which were used directly without further purification.

Static-type cell assembly. Static tests using a CR2032 Coin cell which was assembled in an Ar-filled glove box (H₂O < 0.01 ppm, O₂ < 0.01 ppm). 10 μL catholyte was added into one carbon paper (Ø12 mm) current collector, and an additional piece of carbon paper which was wetted by 15 μL blank electrolyte was placed on the first carbon paper to reduce the loss of active materials. Then, a piece of Celgard 2400 separator (Ø19 mm) was placed on the carbon paper followed by adding 40 μL of blank electrolyte. Finally, a piece of lithium metal (Ø15.6 mm) and nickel foam was placed on the separator.

Flow cell assembly. A self-designed flow battery system is presented in Fig. S1. The flow cells were assembled in the Ar-filled glove box ($\text{H}_2\text{O} < 0.01$ ppm, $\text{O}_2 < 0.01$ ppm) as follows: a piece of lithium metal foil ($\text{Ø}20$ mm) was added into the anode side followed by adding 100 μL electrolyte, and then a Celgard 2400 separator ($\text{Ø}25$ mm) was placed on the surface of the lithium metal foil. For the cathode side, one piece of carbon paper ($\text{Ø}20$ mm) and one piece of graphite felt ($\text{Ø}20$ mm) were added into a polytetrafluoroethylene (PTFE) flow channel ($\text{Ø}25 \times 20 \times 3.0$ mm), and the effective reacting area of the cell is 3.14 cm^2 . The storage tank consists of two tanks (I and II), the solid materials were added into the tank I. Active materials which are soluble in the supporting electrolyte were circulated between the tank and the cell at 12 mL min^{-1} by a peristaltic pump.

Electrochemical analysis. Galvanostatic discharge/charge measurements were performed at room temperature by a battery tester (NEWARE BTS-5V, Neware Technology Co., Ltd.). The cut-off voltage for the static-type cell was set to 1.8-3.0 V. For the Li-S RFB, the cut-off voltage was set to 1.8-3.2 V at the current density ($0.3\text{-}1.0 \text{ mA cm}^{-2}$), 1.7-3.2 V at the current density ($1.5\text{-}2.0 \text{ mA cm}^{-2}$). For the cyclic voltammograms (CV), which were tested between 1.8 and 3.0 V (vs Li/Li⁺) in the static-type cell with the carbon paper as the working electrode, lithium metal was used as counter and reference electrode.

Characterization. Ultra-high-performance liquid chromatography-quadrupole time-of-flight-mass spectrometry (UPLC-QTOF-MS) was used to analyze organic molecules in the self-healing Li-S RFB. UPLC was performed with a Waters Acquity Plus system equipped with an auto-sampler and PDA detector. The separation was obtained on a Waters Acquity UPLC BEH C18 column ($2.1 \text{ mm} \times 100 \text{ mm}$, $1.7 \mu\text{m}$). The solvent phase for UPLC was optimized

as follows: 80%/20% acetonitrile(C_2H_3N)/water (H_2O) (0-2 min), 90%/10% C_2H_3N/H_2O (2-6 min) and the flow rate was 0.2 mL/min. MS analysis was performed on a Waters Xevo G2XS QToF mass spectrometer, which was connected to the UPLC system via an electrospray ionization (ESI) interface. The mass accuracy and reproducibility were maintained by a Lockspray. For this flow cell, 6 mL catholyte consisting of 10 mM PySSPy+10 PhSeSePh, and 6 mg sulfur was added in the tank I. The cell discharged/charged at 0.5 mA cm^{-2} in the voltage range of 1.8-3.2 V. At different stages, 30 μL samples were taken out from the tank II, and were diluted 100 times with C_2H_3N . Then, take 3.0 μL into the UPLC. UV-vis spectra were recorded on a Cary 100 UV-vis spectrophotometer (Agilent). X-ray photoelectron spectroscopy (XPS) was characterized using a 5000 Versa Probe II PS spectrometer equipped with monochromatic Al $K\alpha$ source. Scanning electron microscopy (SEM) was performed on a Zeiss Sigma 500 SEM apparatus. The corresponding flow cell conditions are the same as the cycling test. The elemental mapping was examined with energy dispersive X-ray spectroscopy (EDS) attached to the SEM.

Volumetric Capacity Calculation

The theoretical volumetric capacity of the PySSPy/PhSeSePh solution with/without sulfur in Fig. S10a can be calculated as follows: the volumetric capacity of $1.5 \times 10^{-2} \text{ M}$ PySSPy+PhSeSePh is $7.45 \text{ mAh}/6 \text{ mL} = 1.24 \text{ Ah L}^{-1}$ in the RFB, so, the theoretical volumetric capacity of 1.5 M PySSPy+PhSeSePh can be calculated to be 124 Ah L^{-1} . After adding 150 mg or 200 mg sulfur into the 1 mL 1.5 M PySSPy+PhSeSePh solution, the volumes of the solution become 1.07 mL and 1.1 mL, respectively. So, the contents of sulfur in the catholyte II and III are 140 and 180 g L^{-1} , respectively.

$$V = V_1 + V_s$$

$$V_s = m/\rho$$

Where V is the total volume of the catholyte (mL), V_1 is the volume of PySSPy+PhSeSePh solution (mL), V_s is the volume of solid sulfur power (mL), m (g) and ρ (2.07 g cm^{-3}) represent the mass and density of solid sulfur powder, respectively.

For the 1.5 M PySSPy+PhSeSePh solution with sulfur, the theoretical volumetric capacities of the catholyte **II** and **III** are 332 and 393 Ah L^{-1} , respectively, which can be calculated based on the following formula:

$$\text{Volumetric capacity} = (m \cdot 1543 + 124) / V$$

Where 1543 is the obtained gravimetric capacity of sulfur in the self-healing Li-S RFB (mAh g^{-1}), 124 is the capacity of 1 mL 1.5 M PySSPy+PhSeSePh (mAh), m and v are the same as the above.

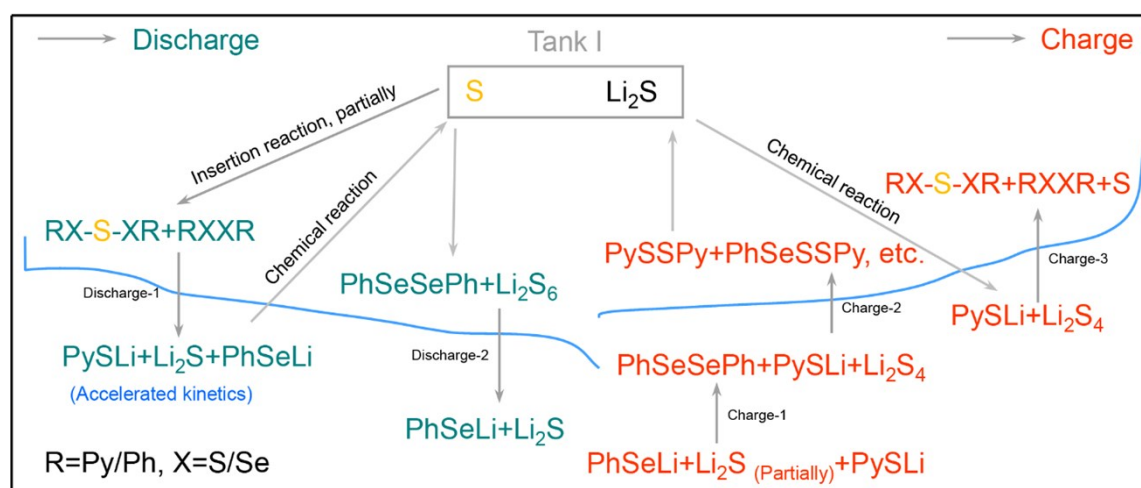


Fig. S1. The main reactions in the self-healing Li-S RFB.



Fig. S2. Solubility test for PySSPy and PhSeSePh. Optical images of PySSPy and PhSeSePh solutions with different concentrations in the supporting electrolyte. For the PySSPy solutions, four bottles were added 44.1, 88.2, 132.2, and 220.3 mg PySSPy, respectively, corresponding concentrations are 1.0 M, 2.0 M, 3.0 M, and 5.0 M, respectively. As for the PhSeSePh solutions, the mass (corresponding concentration) of PhSeSePh in the four bottles are 62.4 (1.0), 93.7 (1.5), 124.8 (2.0), and 187.3 mg (3.0 M), respectively. The volume of electrolyte in every bottle is 0.2 mL. Each sample was stirred for 1 hour before taking pictures.



Fig. S3. Photograph of the self-designed flow battery system. a-c, Assembly process of the flow battery and d, A reservoir with two storage tanks which are linked by a diaphragm and e, A flow battery, f, Digital photograph of a complete flow battery system.

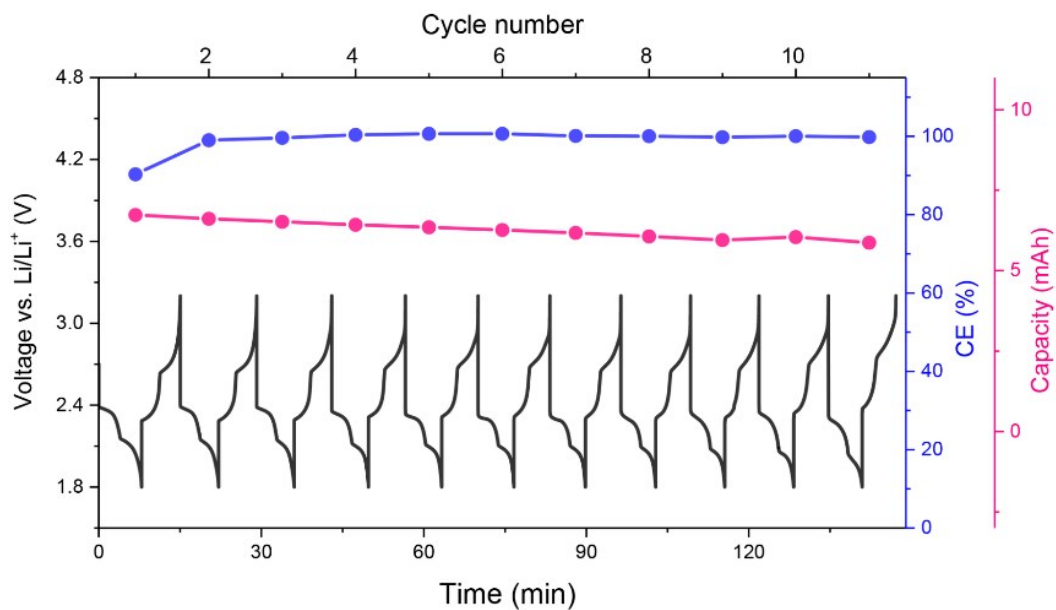


Fig. S4. Capacity retention and voltage curves of the 15 mM PySSPy+PhSeSePh at 0.3 mA cm⁻².

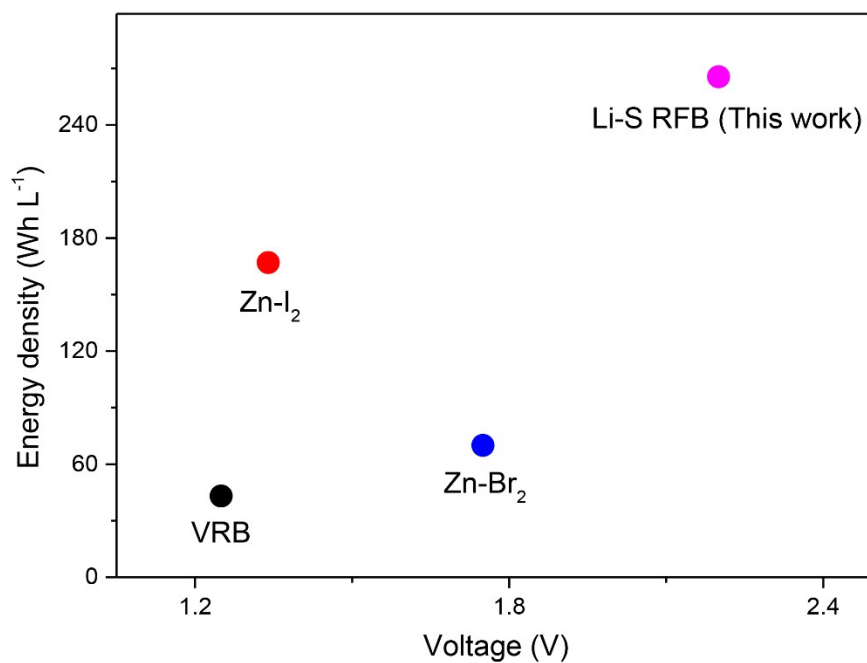


Fig. S5. Comparison of Li-S RFB in this work with some typical aqueous RFBs¹⁻³.

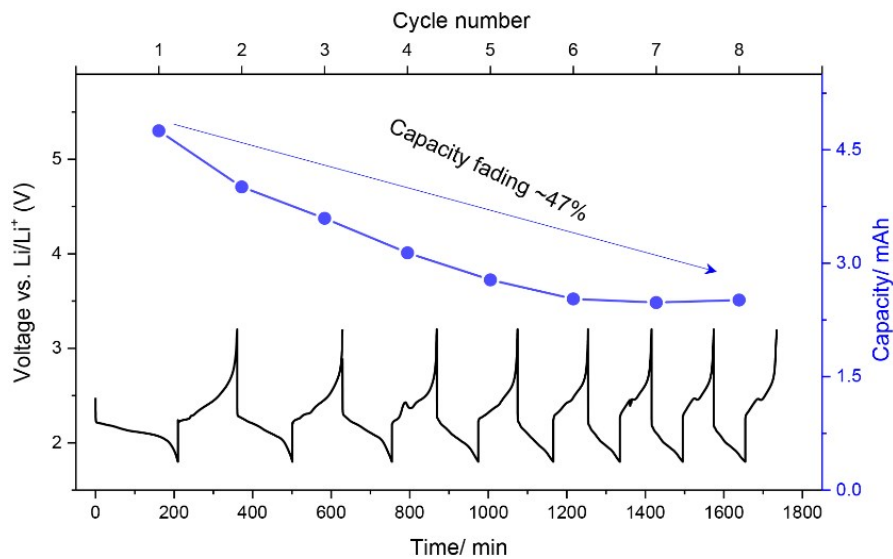


Fig. S6. Capacity retention and voltage profiles of the sulfur-based flow battery with only 5 mg sulfur in the tank at a current density of 0.6 mA cm^{-2} . Due to the low solubility of sulfur in the supporting electrolyte, which requires continuous stirring in tank I .

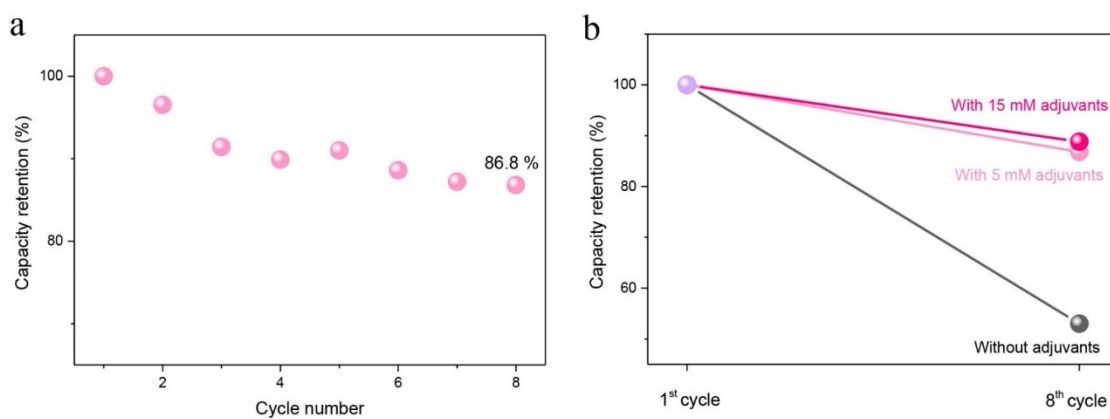


Fig. S7. (a) Capacity retention rate of the Li-S RFB with 5 mM adjvants at 0.6 mA cm^{-2} . (b) Comparison of capacity retention rate of the Li-S RFB with/without adjvants at 0.6 mA cm^{-2} .

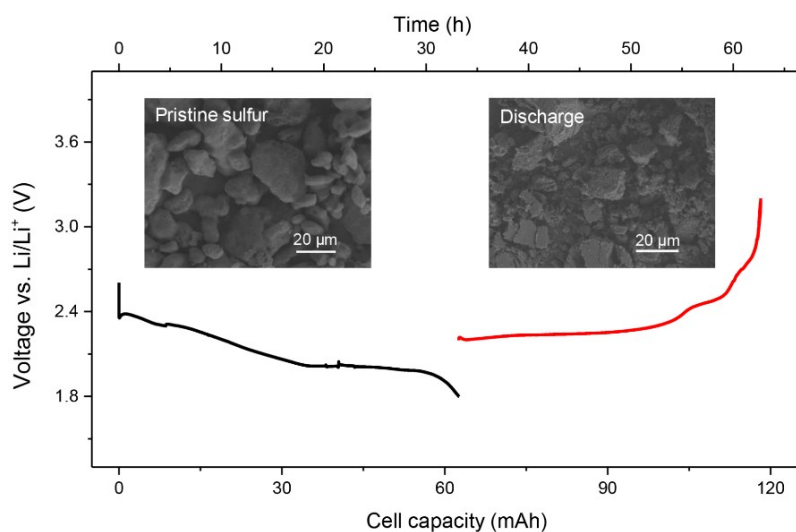


Fig. S8. Relatively high mass loading (27.0 mg cm^{-2}) of active materials was tested in the continuous flow cell at 0.6 mA cm^{-2} , and the inset pictures are SEM images of pristine sulfur and solid particles in tank I after discharging. (PySSPy loading: 6.3 mg cm^{-2} ; PhSeSePh loading: 9.2 mg cm^{-2} ; sulfur loading: 11.5 mg cm^{-2}).

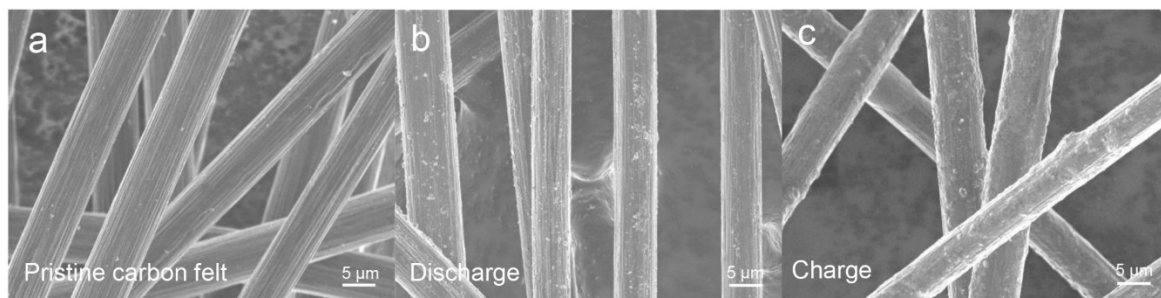


Fig. S9. SEM images of pristine carbon felt (a) and the carbon felt from a fully-discharged/charged flow cell (b/c) at 0.6 mA cm^{-2} . (PySSPy loading: 6.3 mg cm^{-2} ; PhSeSePh loading: 9.2 mg cm^{-2} ; sulfur loading: 11.5 mg cm^{-2}).

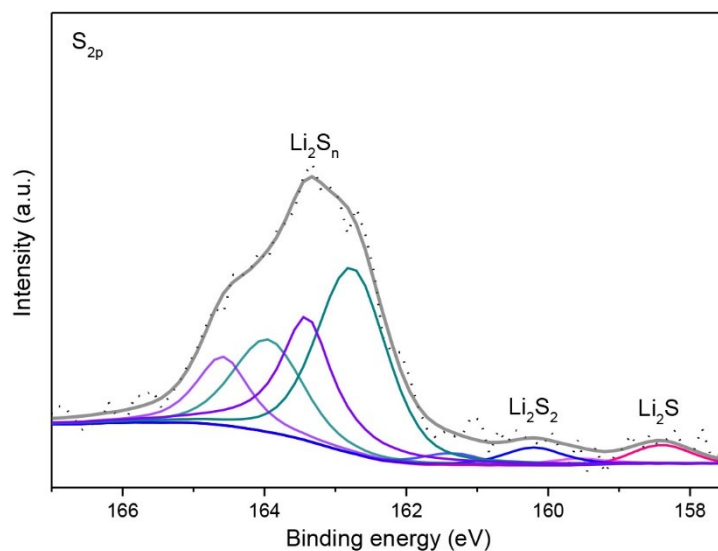


Fig. S10. XPS spectrum of lithium anode without PySSPy/PhSeSePh adjuvants.

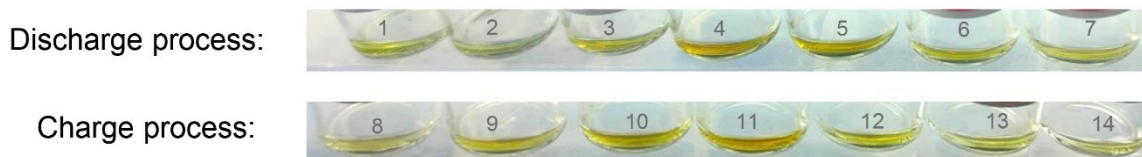


Fig. S11. Photographs of the catholyte at different stages, which were taken from the tank II.

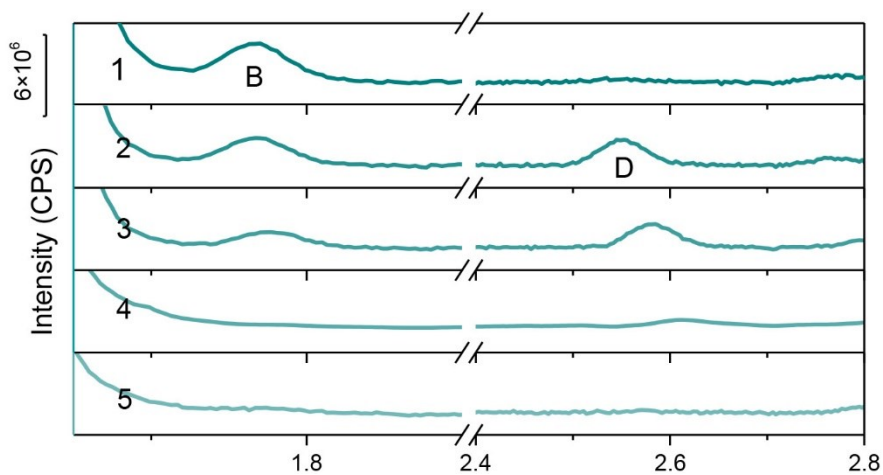


Fig. S12. Partial-enlarged TIC spectra of the catholyte in the discharge process.

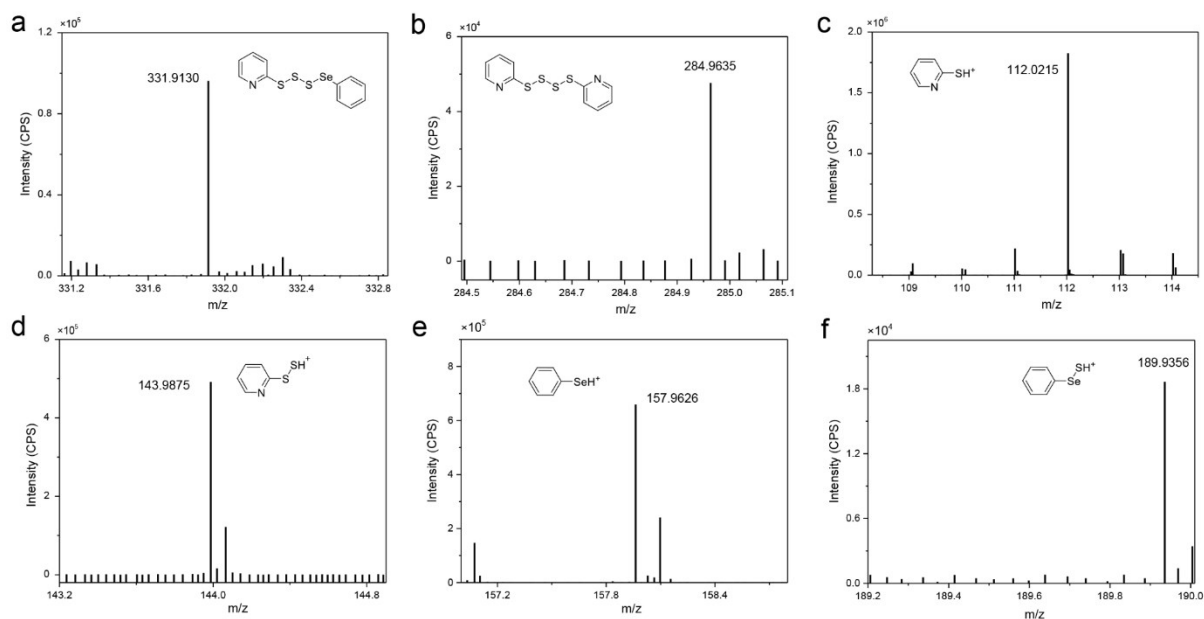


Fig. S13. ESI-MS of PySSSSePh, PySSSSPy, and some discharge/intermediate products.

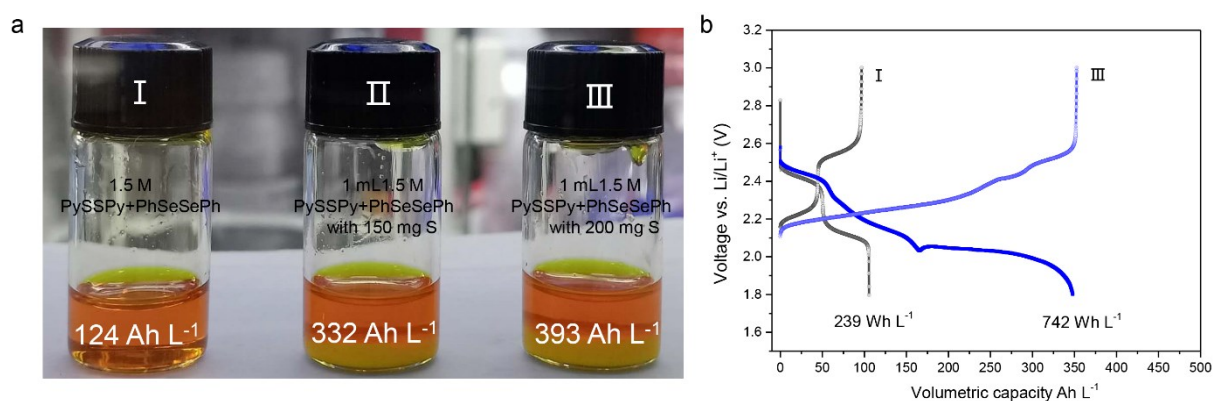


Fig. S14. a, Photographs and corresponding theoretical volumetric capacities of the PySSPy+PhSeSePh solution with/without sulfur in the Li-S RFB and **b,** Volumetric and energy capacities of sample I and III at 0.3 mA cm⁻² in a static-type cell.

Supplementary References

1. B. Li, M. Gu, Z. Nie, Y. Shao, Q. Luo, X. Wei, X. Li, J. Xiao, C. Wang, V. Sprenkle and W. Wang, *Nano Lett.*, 2013, **13**, 1330-1335.
2. B. Li, Z. Nie, M. Vijayakumar, G. Li, J. Liu, V. Sprenkle and W. Wang, *Nat. Commun.*, 2015, **6**, 6303.

3. Q. Z. Lai, H. M. Zhang, X. F. Li, L. Q. Zhang and Y. H. Cheng, *J. Power Sources*, 2013, **235**, 1.